

Influence of long pulse duration on time-resolved laser-induced incandescence

M. Ditaranto · C. Meraner · N. E. L. Haugen · I. Saanum

Received: 8 November 2012 / Accepted: 4 June 2013 / Published online: 16 June 2013
© Springer-Verlag Berlin Heidelberg 2013

Abstract Time-resolved laser-induced incandescence (LII) signal of soot in an ethylene laminar diffusion flame was measured with varying laser pulse durations in the range 50–600 ns. This study presents original results since the majority of LII studies reported are based on 7–10-ns pulse duration. The LII signal from soot is a combination of heating and cooling processes of different time scales, and the influence of the pulse duration is therefore particularly relevant. The most striking finding is that when the pulse durations is longer than approximately 100 ns, the time-resolved LII signal reveals a rebound of the LII signal during its slow decaying part. This feature occurs preferably at high fluence and is unexpected as none of the physical and chemical processes known to control LII signal behaviour, and their models suggest such an effect. The phenomenon occurs with both top hat and near Gaussian temporal laser shapes. Inspection of the time-resolved emission spectra shows no indication of a laser-induced fluorescence effect, although gas-phase PAH generated during the laser heating of soot particles cannot be rejected. Other hypotheses are that the mechanism responsible for that behaviour is linked to a slow rate change of the soot morphological characteristics or to the generation of new particles during the long-duration laser excitation. Finally, experiments show that soot volume fraction measured by integrating the temporal LII signal is not affected by the pulse duration in any regions of the flame, implying that the LII method is applicable with long pulse duration lasers.

1 Introduction

Soot is an unwanted product of combustion because of its harmful impacts on human health and environment. In addition, it is unburned carbon and as such represents a loss of combustion efficiency. Soot is also highly unwanted as it deposits on engine parts and modifies heat transfer properties. Soot is composed of complex chains of carbon atom particles forming aggregates with a fractal-like structure [1]. Primary particles composing soot found in flames have diameters in the range 10–40 nm, while aggregates are on the order of tens to hundreds of nanometres.

Laser-induced incandescence (LII) is a common technique used to locally measure and characterize soot in flames [2]. Although not self-calibrating, the LII method has single-shot capability and is therefore particularly pertinent for use in both laboratory and industrial turbulent flames. When soot absorbs laser light its temperature increases, and as a result, it emits a LII signal according to the black body radiation law. Soon after the start of the laser, the LII signal reaches a peak and then decays due to the negative balance between the global rate of energy production (mainly absorption) and that of energy loss (conduction to the surrounding gas, radiation, loss of mass by vaporization) [3]. Soot volume fraction is measured by integrating the LII signal in tens of nanoseconds range, whereas measuring primary particle diameter requires time-resolved acquisition hundreds of nanoseconds at atmospheric pressure. The LII signal from incandescent soot particles present in the control volume can be measured with a rapid photomultiplier tube or a gated intensified detector. The LII method has been considerably studied during the last 25 years. The modelling of the time-resolved LII signal has focused a lot of interest due to the many physico-chemical processes triggered by laser

M. Ditaranto (✉) · C. Meraner · N. E. L. Haugen · I. Saanum
SINTEF Energy Research, Postbox 4761 Sluppen,
7465 Trondheim, Norway
e-mail: mario.ditaranto@sintef.no

irradiance on the complex soot aggregates. Remaining challenges in that area are described in the review of Schulz et al. [4].

Soot is generated in the flame through a complex series of chemical–physical processes [5] initiated in the fuel-rich region and extending throughout the flame front. To yield valuable information on soot formation in flames, the incandescence process must be generated at a time scale much shorter than the chemical and turbulence time scales, favouring the use of high-energy pulsed lasers. Typically Q-switched Nd:YAG lasers with a pulse duration of 7–10 ns are used, leading to LII signals with a typical duration on the order of hundreds of nanoseconds. However, the signal is generally integrated either close to the LII peak signal (so-called prompt LII) or, although less frequently, over a longer time range of 200–700 ns, to avoid interferences from short lifetime PAH fluorescence. In the latter case, the proportionality of the signal to soot volume fraction is poorer as the contribution from smaller particles (that quickly vaporize) is lower.

Michelsen [6] has investigated the effect of excitation pulse duration with picoseconds lasers in order to explain a process raising unexpectedly the LII signal at the beginning of the excitation, presumably from PAH fluorescence. The question of the effect of longer pulse duration was raised in Schulz et al. [4]. Using CW laser for LII was recently investigated by Black [7], where the preliminary results showed that CW fibre Laser LII depends non-linearly on soot volume fraction and that LII is saturated at 100 W power level, without evidence for soot vaporization. The Single Particle Soot Photometer (SP2) is an apparatus that uses LII to quantify black carbon aerosols [8]. In this technique, described by Stephens et al. [9], light-absorbing refractory aerosol is heated to vaporization by an intense CW laser intracavity beam. LII signal examples given in their work show that graphite particles on the order of 0.5 μm size undergoing 1 MW/cm^2 laser irradiance fully vaporize within 2 μs . The time trace of the LII signals in Stephens et al. [9] seems similar in shape to those with pulsed laser LII, but the size of the particles is one order of magnitude larger than soot primary particle found in flames. On the other hand, Bengtsson and Alden [10] who performed LII study with a 10-ns-duration pulsed laser on in-flame soot, observed that vaporization required a minimum of 10 MW/cm^2 laser irradiance for vaporization to be initiated.

The heating and cooling processes acting on the incandescent particles occur at different time scales. Absorption occurs continuously as long as the laser pulse is active, but its rate decreases as mass is lost by vaporization. Vaporization has the strongest cooling effect and decreases rapidly when the laser light stops. Annealing, which is a process that changes the primary particle microstructure as

a result of heating and vaporization, heats the particle, but since it lowers emissivity, it overall contributes to a decrease in LII signal [3]. Its influence on the LII decay rate is strongly linked to the vaporization process. Long after the pulse (approximately 100 ns), when temperature has dropped below the vaporization point, it is conduction to the surrounding gas that dominates the cooling of soot at atmospheric and high pressure. Although to a lower extent, radiation and oxidation also have cooling and heating effect respectively at similar time scales. Absorption is obviously directly dependent on the pulse duration, and vaporization and annealing are further consequences. Therefore, should the absorption rate be low in the case of long pulse duration, all the processes could compete on the same time scale. A central point to keep in mind during the LII process is that vaporization drives a loss of mass which is known to be very rapid. Many studies (e.g. [1, 3, 4, 11]) have shown with good agreement that significant vaporization of soot occurs at fluence of 0.2 J/cm^2 at 532 nm and that most of the particle is vaporized at higher fluences. Yoder et al. [12] demonstrated in their experiments that the majority of vaporization occurred within the first half of the laser Gaussian temporal profile at fluencies greater than 0.5 J/cm^2 . A slower heat deposition rate on the particles, i.e., longer pulse duration, would allow the cooling mechanisms to balance the vaporization process to a greater extent.

Will et al. [13] discussed the dependency of LII to fluence (J/cm^2) and irradiance (W/cm^2) and commented that for pulse duration on the same order of magnitude as the time scale of the heat transfer processes, irradiance should be more appropriate. Indeed, as long as the laser pulse is shorter than the dominant conductive cooling mechanism time scale, the particles will continue to heat up to the vaporization point depending on the total energy applied, i.e., fluence. But if the absorption rate competes with the global cooling rate, irradiance would better describe when vaporization is reached. To the knowledge of the authors, no LII studies with pulse durations in the range 10 ns–1 μs have investigated the time dependency of these interacting processes. Simulations as those reported in Schulz et al. [4] can be used, but have not been compared to experiments. The present work contributes in filling this gap, by using a laser with varying temporal pulse durations and shapes in a laminar non-premixed ethylene flame. Particular features appearing on the time-resolved profiles at long pulse durations are documented and discussed.

2 Experimental setup

The LII experiments were made on soot particles formed in a non-premixed laminar flame. The burner shown in the

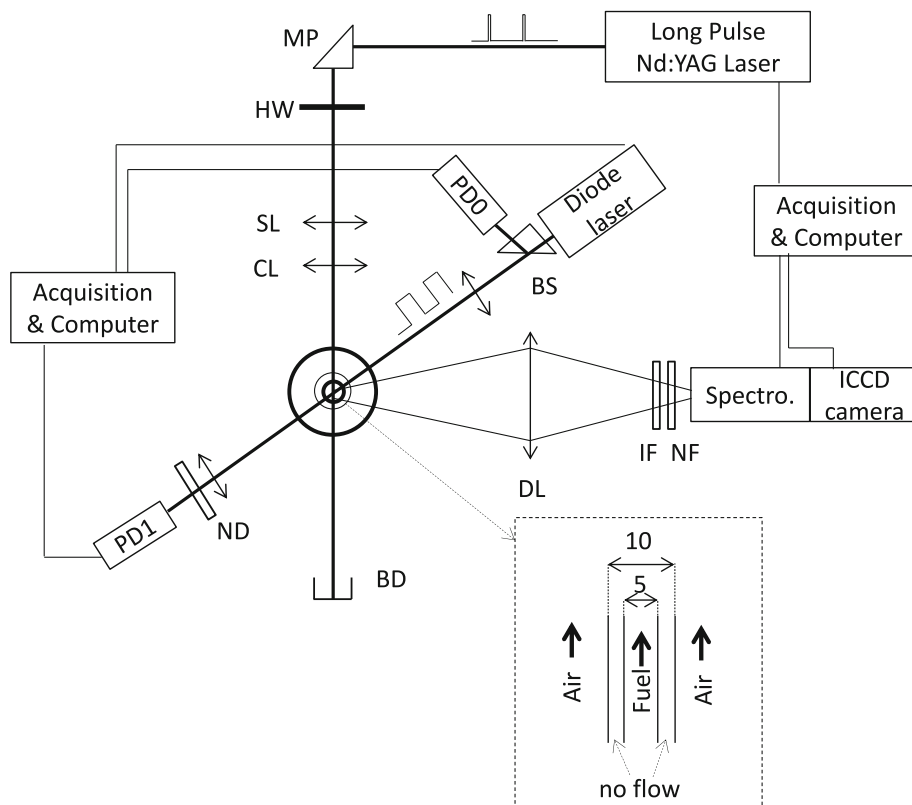
insert of Fig. 1 is a 5 mm diameter circular nozzle for the fuel (ethylene) surrounded by a coaxial tube of 10 mm outer diameter. For that study, the annular channel had no flow. The coaxial tubes are centred in a 97 mm diameter co-flow channel. The flow rate of ethylene was controlled by a thermal mass flow controller at a rate of 0.23 NI/min, corresponding to an exit velocity of 21 cm/s and a Reynolds number of 120. The air is supplied in the co-flow channel at an exit velocity of 23 cm/s. The flame height, defined as the position where soot volume fraction tends to zero, is 95 mm. All the measurements were obtained at a height of 25 mm above the nozzle exit section. Unless stated otherwise, all the time-resolved LII measurements shown are taken at the position of maximum soot volume fraction.

The time-resolved laser-induced incandescence measurements were taken by using a pulsed Nd:YAG laser with temporal shaping capabilities (AGILITE, Continuum). Temporal laser pulse profiles of 50–1,500-ns duration were prepared with both near top hat and Gaussian shapes. The pulse temporal traces captured with a high-speed photodiode from a reflection at the laser head exit are represented on all the LII signal plots in the paper; however, these traces are not synchronized with the represented LII signals. The frequency-doubled laser beam (532 nm) of 3.4 mm $1/e^2$ radius shown in Fig. 1 was directed to the burner through a periscope arrangement followed by a half-wave plate to

restore the beam's vertical polarization, necessary for the measurements involving the use of the spectrograph. The beam was focused with a 1 m focal length spherical lens (SL), combined with a 45 mm focal length cylindrical lens (CL) in order to form a laser sheet. The laser sheet allowed a good spatial resolution in the direction of signal collection, at the expense of high laser fluence. The spatial intensity distribution in the laser sheet was measured at the flame section by traversing a pinhole and a photodiode diode. The laser sheet spread non-homogeneously over a total height of 20 ± 5 mm, and its thickness at the $1/e^2$ waist was 180 ± 25 μm . The values of fluence given in the article are however based on an area of $10 \text{ mm} \times 180 \mu\text{m}$, corresponding to the area where the intensity is concentrated. In addition, the pulse energy was monitored at the laser head and does not take into account the losses in the optical path before reaching the flame (approximately 10–15 % energy loss). Therefore, the fluence values given throughout the paper must be considered as estimates.

The LII signal was imaged with a 1:1 magnification on the photocathode of an intensified CCD camera or spectrograph entrance slit with a large diameter 250 mm focal length lens. The Mie/Rayleigh scattering from soot and gas and reflections were rejected by the use of a notch filter (NF) centred on the laser line. To minimize the interferences from molecular fluorescence and other excited radical emission, a 10-nm band-pass filter (IR) centred at 488 nm

Fig. 1 Sketch of the experimental set-ups for LII and LBE methods (in the same sketch for conciseness, but not used simultaneously). *Insert* burner nozzle dimensions. Abbreviations explained in text



was also placed in the collection path. For spectrally resolved measurement, a 300 mm focal length spectrograph was placed in front of the ICCD camera. The spectrograph-camera system was not calibrated. With this detection arrangement, the complete radial profile through the flame could be measured simultaneously. The radial profiles were obtained by averaging 10 pixel rows, corresponding to a spatial resolution of roughly 260 μm in the stream-wise direction and 26 μm in the lateral direction. The time-resolved LII signals were reconstructed by gradually sliding a 10-ns intensification gate without overlapping from the start of the laser pulse. At each time step, 10 shots were accumulated directly on the CCD chip. For the spectrally resolved measurements, the signal levels were lower, thus different settings had to be used: 40 on-CCD accumulations of a 20 ns intensification gate. The signal intensity of the LII plots presented is not calibrated (given in arbitrary units), but they are comparable with each other.

The soot volume fraction was calibrated by using the laser beam extinction method (LBE). The LBE set-up is also shown in Fig. 1, where a 635 nm CW laser diode was pulsed at 200 Hz. One measurement point consisted in acquiring simultaneously the laser signals before (on photodiode PD0) and after (on photodiode PD1) the beam crossed the flame, and at two consecutive low-high states of a laser cycle. This allowed to correct the extinction measurement for both laser intensity variation and flame luminosity fluctuations. Extinction measurements were averaged over typically 5,000 laser cycles at each radial position through the flame. LBE is a line-of-sight integrated technique, but because of the symmetric and laminar configuration used, a three-point Abel deconvolution could be used to retrieve soot volume fraction radial profiles through the flame. The LII and LBE measurements were not performed simultaneously.

3 Results and discussion

A so-called fluence curve is shown in Fig. 2 for a laser pulse duration of 200 ns. The integrated LII signal reaches a plateau for pulse energies measured at the laser head above 30 mJ. Based on the dimension of the laser sheet thickness described in §2, this value corresponds to a fluence (approximately 1.7 J/cm^2) greater than the widely reported value of 0.2 J/cm^2 for 532 nm excitation (e.g. [1, 3, 4, 11]). Because of the large uncertainties on the actual laser energy at the flame location and the non-homogeneous intensity profile of the laser sheet, we will refer in the remainder to the value of 30 mJ at which the plateau, characteristic of intense vaporization, is reached. In this section, we present results obtained with different pulse configurations. The laser pulse duration is varied, first by

keeping the peak energy constant and secondly by keeping the total pulse energy constant (therefore by adapting the peak energy). The last tests consist in increasing the pulse energy at constant pulse duration. Emission spectra are then investigated looking for possible spectral features, and finally, the use of long laser pulse duration on soot volume fraction measurement is discussed.

3.1 Influence of laser pulse duration on LII signal

Figure 3 shows the evolution of the LII signal, when the temporal top hat laser pulse duration is increased from 50

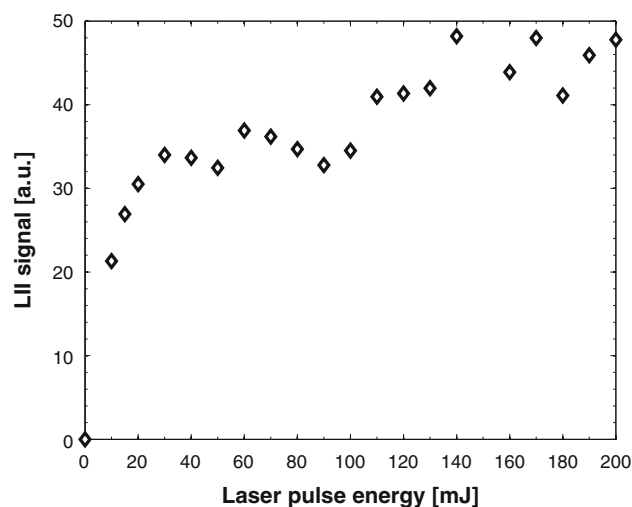


Fig. 2 LII signal integrated over 600 ns as a function of laser pulse energy with a pulse duration of 200 ns. Threshold point occurs at laser energy of approximately 30 mJ corresponding to the intense vaporization of soot

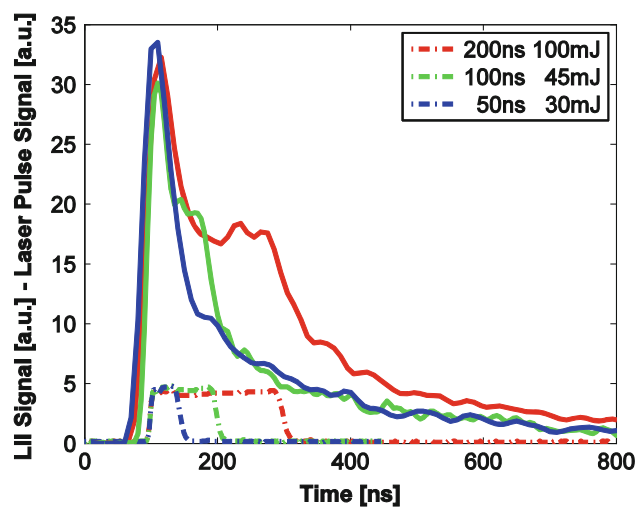


Fig. 3 Time-resolved LII signals (*solid lines*) obtained at varying laser pulse durations and constant laser peak energy. As pulse duration increases a shouldering (at 100 ns) and eventually a rebound of the LII signal (at 200 ns) occur. *Dashed lines* show the laser pulse profiles, not synchronized with the LII signals

to 200 ns while keeping the peak energy constant. The increase in pulse duration is thus equivalent to an increase in total energy or fluence. At the start of the pulse, the LII signal builds up equally for all cases, as a result of particles absorbing laser energy and heating up (the differences in peak height may be due to the finite gating at each time step, hence to the averaging effect in a region of strong gradient). After the LII peak signal is reached, the particles start to transfer energy out (cool) at a rate which is higher than heating by the absorbed laser light. The dominant cooling mechanism at this stage is the loss of mass that occurs during vaporization. For the 50 ns pulse, the LII signal is continuing to decay as expected at a rate dependent on the primary particle diameter. When the pulse is kept active longer at equal peak energy (see 100 ns curve), one observes a sudden decrease in the decay rate after approximately 50 ns. This observation is unexpected as increasing the fluence is known to increase the decay rate as a result of an increase in vaporization rate [3], with the effect of narrowing the LII signal through a steeper decay of the LII signal. This first observation indicates that the effect of laser fluence on LII has a dependency on the time scale of the excitation.

A further increase in pulse duration to 200 ns shows not only a further delay in the decay, but also an increase of the LII signal, occurring in the form of a rebound. The cause of this phenomenon is unclear as none of the processes known to take part in the laser-induced incandescence theory [3] predicts such an effect. The initial decay of LII is due to vaporization (mass loss) which contributes mostly to the drop in the incandescence signal. The decay due to heat conduction and radiation has longer time scales, but vaporization would still be dominant if the pulse is active longer. According to the known processes controlling LII, a secondary increase in the LII signal would require that the soot particles size increases or that the morphology of soot changes (through fractal dimension of the aggregates for example), or as suggested in Michelsen et al. [14] that new particles are created out of the carbon clusters generated by vaporization and photo desorption. However, these effects would have to be large enough to outweigh the mass loss by vaporization which seems improbable for the two first hypotheses. Michelsen et al. [14] evidenced formation of new particles above 0.12 J/cm^2 at 532 nm and showed that their number density and size (always lower than the original primary particles) increase with fluence. This could be a possible explanation, but since high fluence LII with traditional 7–10 ns laser pulse has not evidenced such an increase in LII signal, that would indicate that the processes responsible for new particles generation are enhanced at longer pulse duration. Worth noting is that Michelsen et al. [14] showed that particles are not created by breaking apart from aggregates.

The rebound phenomenon was observed to appear around 100 ns after the LII signal peak when using a 200 ns pulse duration at both 100 mJ and 528 mJ total pulse energy, i.e. at fluences well within the vaporization regime (cf. Fig. 2); therefore, this effect is unlikely the result of accumulated energy during the pulse. Witze et al. [11] show an example of experimental LII signal with some similitude, where a slight increase in the LII signal can be observed. The authors do not propose an explanation, but Michelsen et al. [15] later attributed this effect to a possible ghost LII signal from out of focus soot particles because of the large beam used and the non-homogeneous spatial profile of the excitation source. Interestingly enough, the predictions shown in Michelsen [3] with their base model exhibit a similar effect at high fluence, but not in their experiments.

The depicted behaviour is observable with both a top hat and quasi-gaussian pulse temporal profile as shown on Fig. 4, therefore rejecting an eventual effect of the temporal profile of the laser beam.

In an effort to eliminate potential interferences, several experimental configurations were tested. For example, a test was made by removing the lenses SL and CL (cf. fig. 1) and placing a 3 mm diameter holes in the beam path. In so doing, the laser sheet was replaced by an unfocused laser beam which wings were removed. The same behaviour as a function of pulse duration was observed. Another probable interference could come from fluorescence superimposed on the incandescence signal. Such an effect is well known and reported in, for example Bengtsson et al. [10] and discussed in Michelsen [6]. The laser-induced fluorescence signal would originate from PAH present in

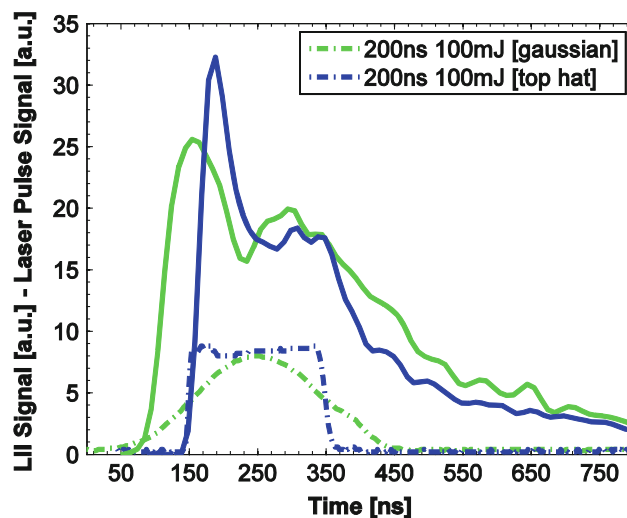


Fig. 4 Effect of laser pulse temporal shape on LII. Time-resolved LII signals (*solid lines*) obtained with a top hat and near Gaussian laser pulse temporal shapes (*dashed lines*, not synchronized with the LII signals)

the gas phase and is intermediate species in the soot formation mechanism. Further discussion on that possible signal interference is provided in the following sections.

3.2 Influence of fluence on long pulse LII signal

To further investigate the rebound behaviour, a set of measurements at constant total pulse energy, but varying pulse duration is presented in Fig. 5. In this experiment, the peak intensity of the laser energy had to be adapted to each pulse duration in order to keep the total energy constant. The same features as previously discussed are visible, namely a delay in the LII signal decay for pulses longer than around 100 ns, and a clear rebound of the LII signal as the pulse duration further increases. The temporal resolution of the LII signal measurement is limited by the 10 ns gating time of the intensifier; therefore, it is not possible to estimate precisely at which pulse duration such an effect already occurs. In our experiments, the shortest pulse duration revealing a shouldering of the signal was 75 ns.

In the cases shown in Fig. 5, the fluence is approximately three times the threshold value for the plateau observed in Fig. 2. The fluence calculated with the limitation discussed previously (cf. §2) is on the order of 5 J/cm^2 , and the irradiance varies from 9 to 110 MW/cm^2 for the 600 and 50 ns pulse, respectively. In terms of fluence, these conditions are well above the accepted threshold at which the vaporization regime starts with a 532 nm excitation, but only the case at 50 ns is above the irradiance threshold of 20 MW/cm^2 reported by Bengtsson et al. [10]. There is however no doubt from the shape of LII signals in Fig. 5, that vaporization has occurred (presence of characteristic sharp decrease in signal after the peak,

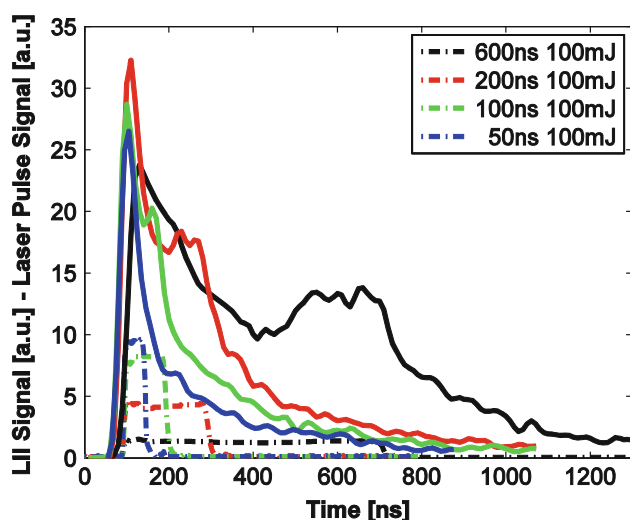


Fig. 5 Time-resolved LII signals (solid lines) obtained at varying laser pulse durations and constant laser total energy. Dashed lines show the laser pulse profiles, not synchronized with the LII signals

instead of slow decay dominated by conduction). These results highlight the need for a better characterization of the different LII regimes as a function of laser pulse duration other than the commonly 7–10-ns pulse used.

Most of the studies on both temporally resolved and integrated LII are based on either Nd:YAG or Nd:YAG-pumped lasers with a pulse duration of 7–10 ns. In these conditions, varying laser fluence (J/cm^2) is solely done by varying the pulse energy. Following the same approach, the laser fluence was varied at constant pulse durations. For a pulse duration of 50 ns as shown in Fig. 6a, the LII signal does not exhibit any unexpected shape. The peak LII signals at 30 mJ and 100 mJ pulse energy are comparable truly because the vaporization regime is reached. For the longer pulse cases of Fig. 6, the rebound of the LII signal is clearly apparent above a given pulse energy threshold. At all the lowest energy cases, it seems that no significant vaporization has occurred and the cooling process is mainly controlled by the low-rate conduction to the surrounding. Occurrence of the rebound seems therefore to require a minimum duration of the active pulse and a certain degree of vaporization. Further observations indicate that neither the position in time of the rebound or its signal intensity is affected by the fluence, excluding a correlation of the phenomenon to the amount of energy absorbed.

3.3 Spectrally resolved long pulse LII

All time-resolved measurements presented were collected at 488 nm with a 10-nm-wide band-pass filter, and the elastic scattering (Rayleigh/Mie and reflections) was strongly rejected with a notch filter. This is a common configuration in LII in order to avoid unwanted excited radicals (as C_2) emission which are formed during the soot vaporization [10] and fluorescence from PAH which are precursors in the soot formation mechanism. PAH were shown by Michelsen [3, 6] to contribute to the LII signal at a very early stage, due to the short lifetime of fluorescence. In order to exclude any effects of molecular interferences from the observed rebound behaviour in long pulse LII, spectrally and time-resolved LII measurements were taken.

The lower panel of Fig. 7 shows a LII signal time trace marked by vertical lines. Each vertical line corresponds to the time at which a spectrum was taken and shown on the upper panel. Albeit noisy due to the short gating time, the non calibrated spectra of Fig. 7 show good spectral structure continuity throughout the LII process, with no apparent presence of molecular band structures. The same measurements were repeated with the complete filtering scheme (i.e. notch filter and interference filter) and are shown in the same graph (dashed lines) appearing as short spectral windows. The filtering scheme chosen has a good

Fig. 6 Time-resolved LII signals (*solid lines*) obtained at increasing laser pulse energy and constant pulse duration: **a** 50 ns; **b** 100 ns; **c** 200 ns; and **d** 600 ns. *Dashed lines* show the laser pulse profiles, not synchronized with the LII signals

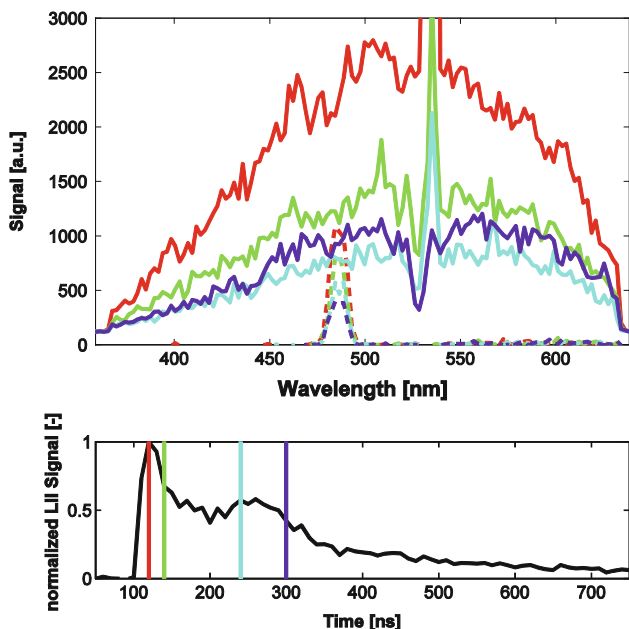
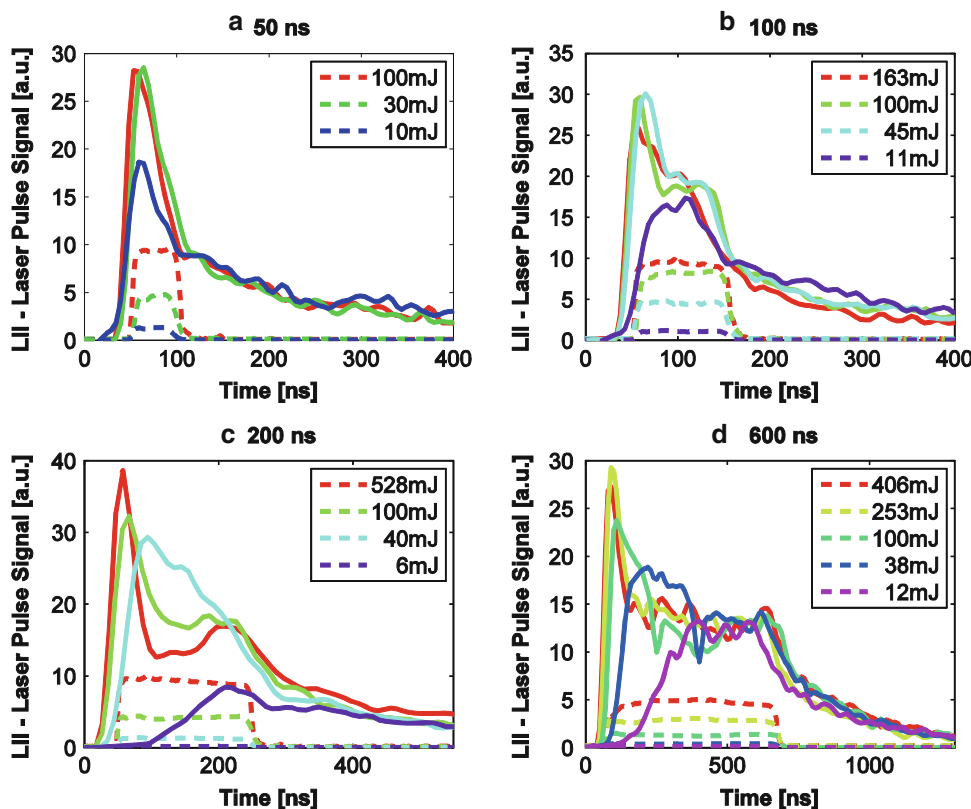


Fig. 7 Non-calibrated spectra obtained at different times during the LII signal with a 20 ns gating time. *Lower panel* shows the time-resolved LII signal with *vertical lines* indicating at which time position the spectra were taken. Corresponding spectra (*solid lines*) are shown in the *upper panel*. *Dashed lines* in the *upper panel* are spectra taken with the complete filtering scheme

efficiency with a high rejection ratio of all features outside the spectral window. For example, the strongest peak at 535 nm, which is a wing of the elastic scattering leaking through the notch filter, is not participating in the LII signal collected. PAH fluorescence can be induced (LIF) by the 532 nm excitation for very long chains or by two-photon excitation of shorter PAH chains. It has a very broadband emission and could contribute significantly to the continuum [6].

The air side of the laminar diffusion flame has low or no PAH [16]. Measurements were taken throughout the entire radial profile of the flame and the rebound feature appeared irrespective of the position in the flame, on both the fuel-rich and air-rich sides. This a priori excludes LIF of PAH to be responsible for the rebound signal. However, we should not ignore PAH or other molecules which coat the soot particles to be dispersed during laser-induced vaporization. But, if long-chained molecules were generated during vaporization, the phenomenon would probably occur quite early after the LII peak, especially at high fluences, as indeed, it is well established that high particle volume reduction is achieved before the end of the laser pulse [11, 12]. The LII time series obtained at highest fluences for the longest pulses in Fig. 6c, d are clear indication that on the hypothesis of early generated PAH by soot vaporization, the time delay is too long as compared to the nanosecond time scale of excited PAH

lifetimes. Therefore, laser-induced PAH fluorescence is not our privileged explanation.

3.4 Practical implications for the measurement of soot volume fraction

Soot formation is the result of a sequence of complex steps involving precursor formation, particle inception, growth, and balanced by oxidation [5]. The rate of formation is strongly dependent on the local temperature and species concentrations. In the non-premixed laminar flame studied, there is a clear transition between the fuel side and the air side with no influence of local turbulence. Therefore, the soot formation progress in the present diffusion flame is only a function of the local position throughout the flame front. Measuring the LII signals at different positions would as a result reveal whether the progress in soot growth and structure (size and shape of the aggregates) would affect the LII signal trace when the pulse duration is long. As discussed previously, examination of the time-resolved LII signals (not shown for consistency) at various positions in the flame and for various pulse durations did not show any qualitative differences. One can conclude that firstly there is no correlation between the local structural characteristics of soot in a diffusion flame and the rebound phenomenon, and secondly that LII measurements with long pulse excitation are not biased by the soot characteristics.

The study shows that in addition to the many experimental factors described in Michelsen [3], the pulse duration is also influencing the behaviour of the time-resolved

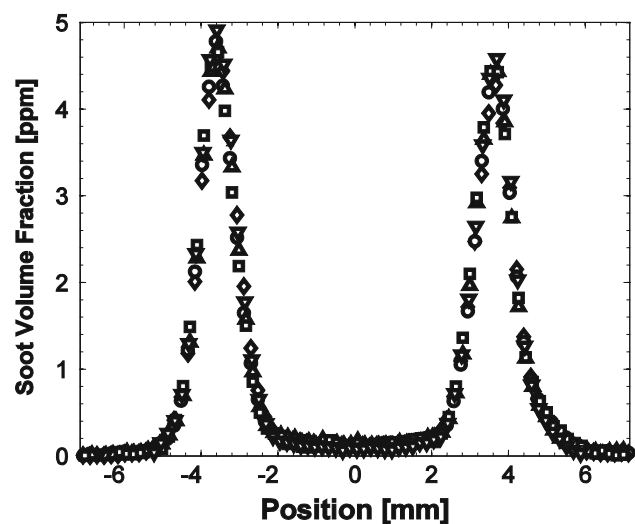


Fig. 8 Radial profiles of soot volume fraction across the flame at 25 mm above the nozzle exit plane, measured by integrated LII with varying laser pulse durations: \square : 50 ns, top hat; Δ : 100 ns, top hat; \circ : 200 ns, top hat; ∇ : 200 ns, Gaussian; \diamond : 600 ns, top hat

LII signal. An important question is whether lasers other than the traditional Q-switched YAG laser are suitable for LII measurement. Radial profiles of soot volume fraction obtained by integrating the LII signal until it reaches 5 % of its peak value are shown in Fig. 8. Pulse durations span from 50 to 600 ns, all with top hat temporal shapes, but one which has a Gaussian-like shape. The integrated LII signal at each pulse duration case was calibrated by the LBE method. Owing to the inaccuracies caused by the sliding gate and consequent averaging effect, all the profiles irrespective of the pulse duration and shape can be considered to coincide fairly well. Therefore, the pulse duration of the excitation source does not seem to bias the measurement of soot volume fraction by integrated LII, further meaning that applying LII with lasers having long pulse characteristics as, e.g., kHz Cu vapour laser and eventually CW laser diodes is possible.

4 Conclusions

The study has shown that the measurement of soot volume fraction by LII is not impaired by the use of pulse durations in the range 50–1,000 ns. This result opens for the use of a broader variety of lasers in LII. On the other hand, the time-resolved LII measurements showed an unexpected behaviour for pulse longer than approximately 100 ns, where a rebound of the LII signal appeared. The phenomenon is seen to be only dependent on the time scale of the excitation and not on the energy absorbed. Measurements on each side of the laminar diffusion flame front suggest that the phenomenon is not related to the primary soot characteristics or presence of PAH, although gas-phase PAH generated during the laser heating of soot particles cannot be rejected. It is further investigated by spectrally resolved measurements that no apparent laser-induced effects is interfering with the collected signals. The established understanding of the thermal processes controlling LII cannot explain this behaviour unless a dramatic change of soot morphological characteristics occurs during the long duration excitation. Although not validated in this study, hypotheses could be formation of new particles from nuclei formed during the excitation process, or a slow rate morphological change of soot during long excitation. The next objective is to identify the physical process responsible for that unexpected LII signal rebound in long-duration laser excitation in order to improve the predictive models used and the measurement of particle soot characteristics.

Acknowledgments This publication has been produced with support from the BIGCCS Centre, performed under the Norwegian research program Centres for Environment-friendly Energy Research

(FME). The authors acknowledge the following partners for their contributions: Aker Solutions, ConocoPhillips, Gassco, Shell, Statoil, TOTAL, GDF SUEZ and the Research Council of Norway (193816/S60).

References

1. R.L. Vander Wal, T.M. Ticich, A.B. Stephens, *Appl. Phys. B* **67**, 115 (1998)
2. L.A. Melton, *Appl. Opt.* **23**, 2201–2208 (1984)
3. H.A. Michelsen, *J. Chem. Phys.* **118**, 7012–7045 (2003)
4. C. Schulz, B.F. Kock et al., *Appl. Phys. B* **83**, 333–354 (2006)
5. I.M. Kennedy, *Prog. Energ. Combust. Sci.* **23**(2), 95–132 (1997)
6. H.A. Michelsen, *Appl. Phys. B* **83**, 443–448 (2006)
7. J.D. Black, *Laser Applications to Chemical, Security and Environmental Analysis*, OSA Technical Digest Series (CD) paper LWB5. Optical Society of America (2010)
8. J.P. Schwarz et al., *J. Geophys. Res.* **111**, D16207 (2006). doi: [10.1029/2006JD007076](https://doi.org/10.1029/2006JD007076)
9. M. Stephens, N. Turner, J. Sandberg, *Appl. Opt.* **42**, 3726–3736 (2003)
10. P.E. Bengtsson, M. Alden, *Appl. Phys. B* **60**(1), 51–59 (1995)
11. P.O. Witze, S. Hochgreb et al., *Appl. Opt.* **40**(15), 2443–2452 (2001)
12. G.D. Yoder, P.K. Diwakar, D.W. Hahn, *Appl. Opt.* **44**, 4211 (2005)
13. S. Will, S. Schraml, K. Bader, A. Leipertz, *Appl. Opt.* **37**(24), 5647–5658 (1998)
14. H.A. Michelsen, A.V. Tivanski, M.K. Gilles et al., *Appl. Opt.* **46**, 959–977 (2007)
15. H.A. Michelsen, P.O. Witze et al., *Appl. Opt.* **42**(27), 5577–5590 (2003)
16. C.R. Shaddix, K.C. Smyth, *Combust. Flame* **107**(4), 418–452 (1996)